

Spectral Analysis of Jet Substructure with Neural Networks: Boosted Higgs and Sgluon Case

Sung Hak Lim



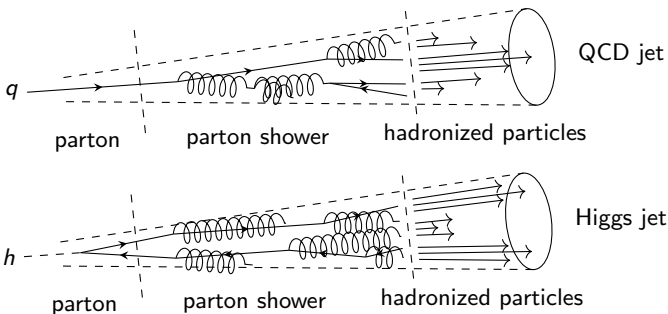
Beyond the BSM, Ikaho Onsen, Gunma, Japan

Oct. 2018

based on S. H. Lim, M. M. Nojiri, arXiv:1807.03312, submitted to JHEP
A. Chakraborty, S. H. Lim, M. M. Nojiri, work in progress

Jets and Boosted Particles

- At a hadron-hadron collider, such as LHC, a collimated particle cluster called a jet often appears when a colored parton is produced.
- As LHC stacking up multi TeV center-of-mass energy events, boosted heavy particles is produced and form a single collimated cluster of particles similar to the QCD jets. ($m_{EW}/\sqrt{\hat{s}} = \mathcal{O}(0.1)$)



- We have to differentiate these non-QCD jets from QCD jets to maximize sensitivity of channels involving boosted particles.

Jet Substructure !

A Catalog of Observables of Jet Substructure

There are lots of observables of jet substructure, which are focussing on particular substructure. A few examples are:

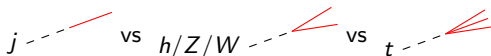
mass of the mother particle:

m_{jet} , trimmed m_{jet} , ...



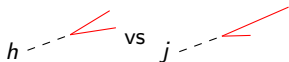
n -prong jet:

n -subjettiness ratio, D_2 , ...



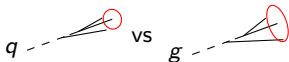
subjettiness p_T asymmetry:

mass drop tagger, ...



color charge:

jet girth, ...



color flow:

jet pull between subjets, ...



A Catalog of Observables of Jet Substructure

There are lots of observables of jet substructure, which are focussing on particular substructure. A few examples are:

mass of the mother particle:

m_{jet} , trimmed m_{jet} , ...



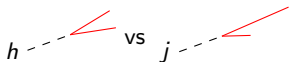
n -prong jet:

n -subjettiness ratio, D_2 , ...



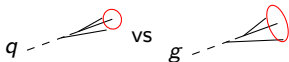
subjettiness p_T asymmetry:

mass drop tagger, ...



color charge:

jet girth, ...



color flow:

jet pull between subjets, ...



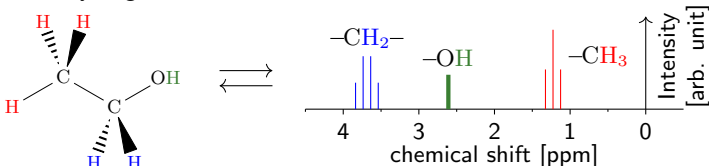
Q: is there any generic framework which is highly visual and unifies these analyses?

- I want to introduce an analogy from

¹H-NMR Analysis in Organic Chemistry.

A Spectral Function from Analogy of Jet Substructures and $^1\text{H-NMR}$ Analysis in Organic Chemistry

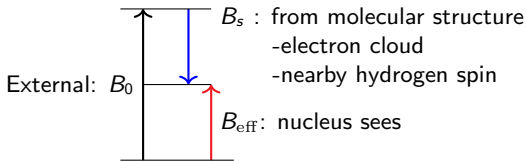
- The $^1\text{H-NMR}$ spectrum can be used for identifying the topological skeleton of an organic molecule, the carbon skeleton, from interaction between hydrogen nuclei and the rest of molecular structure.



- Chemical shift (δ): a resonant frequency of precession relative to a reference in a magnetic field.

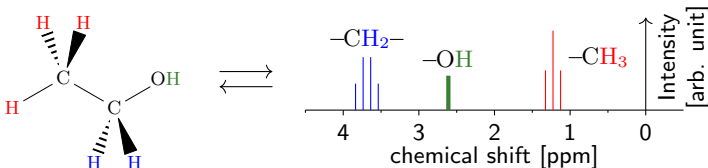
$$\nu = \frac{\gamma}{2\pi} B_{\text{eff}}, \quad B_{\text{eff}} = B_0 + B_s$$

$$\delta = \frac{\nu_{\text{sample}} - \nu_{\text{ref}}}{\nu_{\text{ref}}}$$

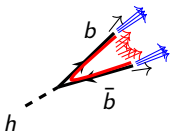


A Spectral Function from Analogy of Jet Substructures and $^1\text{H-NMR}$ Analysis in Organic Chemistry

- The $^1\text{H-NMR}$ spectrum can be used for identifying the topological skeleton of an organic molecule, the carbon skeleton, from interaction between hydrogen nuclei and the rest of molecular structure.

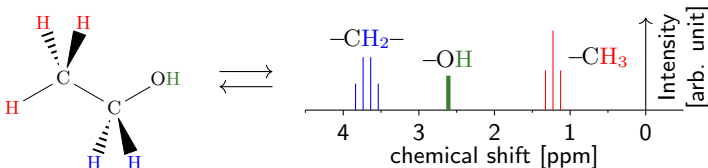


- Jets also have a topological skeleton, the originating partons.

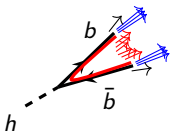


A Spectral Function from Analogy of Jet Substructures and $^1\text{H-NMR}$ Analysis in Organic Chemistry

- The $^1\text{H-NMR}$ spectrum can be used for identifying the topological skeleton of an organic molecule, the carbon skeleton, from interaction between hydrogen nuclei and the rest of molecular structure.



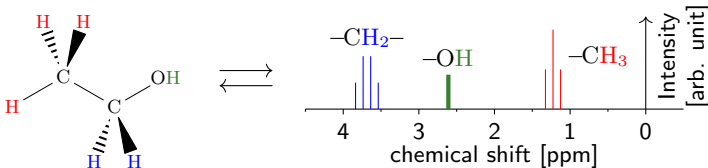
- Jets also have a topological skeleton, the originating partons.



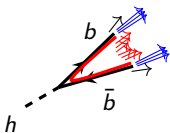
- Can we build a similar analysis framework of jet substructure to identify the originating partons of the jet?

A Spectral Function from Analogy of Jet Substructures and $^1\text{H-NMR}$ Analysis in Organic Chemistry

- The $^1\text{H-NMR}$ spectrum can be used for identifying the topological skeleton of an organic molecule, the carbon skeleton, from interaction between hydrogen nuclei and the rest of molecular structure.



- Jets also have a topological skeleton, the originating partons.

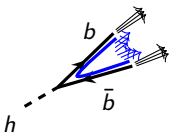
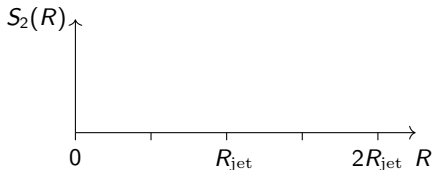


- To measure correlation between jet constituents, we define an IRC safe binned spectral function of angular distance R ,

$$S_2(R; \Delta R) = \frac{1}{\Delta R} \sum_{\substack{i,j \in \text{jet} \\ R_{ij} \in [R, R+\Delta R]}} p_{T,i} p_{T,j}$$

A typical Higgs jet

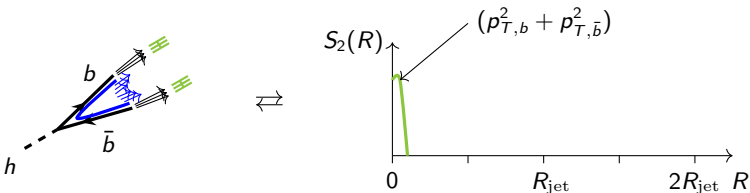
- The spectrum contains information on non-local correlation in the jet.


 \Leftrightarrow


$$S_2(R; \Delta R) = \frac{1}{\Delta R} \sum_{\substack{i,j \in \text{jet} \\ R_{ij} \in [R, R+\Delta R]}} p_{T,i} p_{T,j}$$

A typical Higgs jet

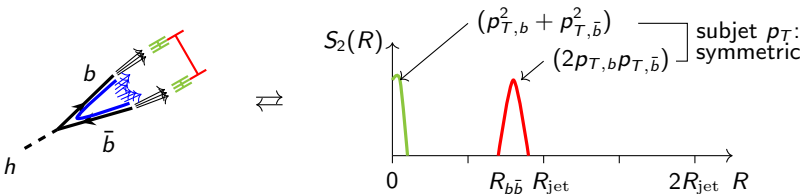
- The spectrum contains information on non-local correlation in the jet.



$$S_2(R; \Delta R) = \frac{1}{\Delta R} \sum_{\substack{i,j \in \text{jet} \\ R_{ij} \in [R, R+\Delta R]}} p_{T,i} p_{T,j}$$

A typical Higgs jet

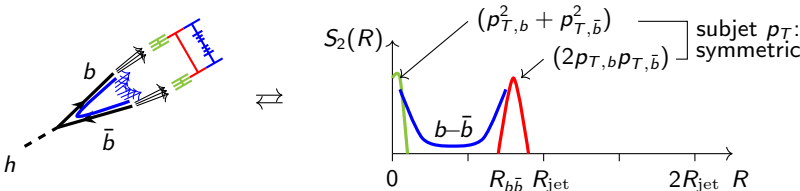
- The spectrum contains information on non-local correlation in the jet.



$$S_2(R; \Delta R) = \frac{1}{\Delta R} \sum_{\substack{i,j \in \text{jet} \\ R_{ij} \in [R, R+\Delta R]}} p_{T,i} p_{T,j}$$

A typical Higgs jet

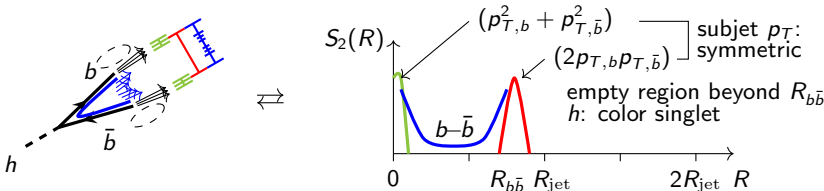
- The spectrum contains information on non-local correlation in the jet.



$$S_2(R; \Delta R) = \frac{1}{\Delta R} \sum_{\substack{i,j \in \text{jet} \\ R_{ij} \in [R, R+\Delta R]}} p_{T,i} p_{T,j}$$

A typical Higgs jet

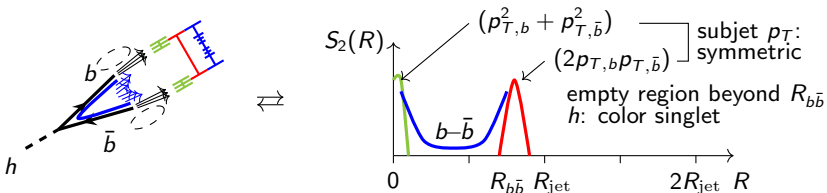
- The spectrum contains information on non-local correlation in the jet.



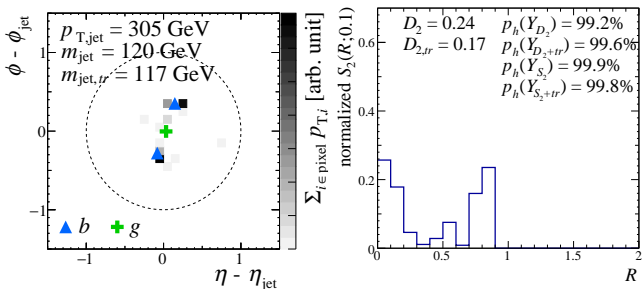
$$S_2(R; \Delta R) = \frac{1}{\Delta R} \sum_{\substack{i,j \in \text{jet} \\ R_{ij} \in [R, R+\Delta R]}} p_{T,i} p_{T,j}$$

A typical Higgs jet

- The spectrum contains information on non-local correlation in the jet.

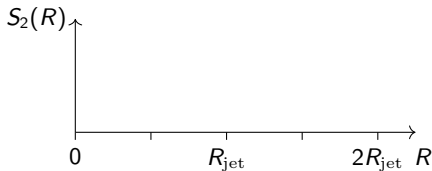
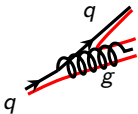


- This is a typical Higgs jet from MG5_aMC@NLO+Pythia8+Delphes.



A typical QCD jet

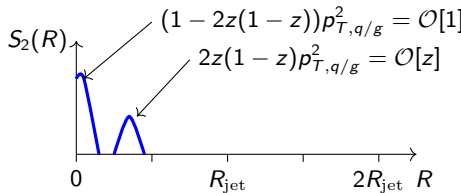
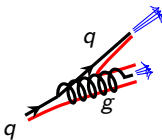
- Meanwhile, a typical QCD jet has a smoothly falling behavior according to the parton splitting kernels.



$$S_2(R; \Delta R) = \frac{1}{\Delta R} \sum_{\substack{i,j \in \text{jet} \\ R_{ij} \in [R, R+\Delta R]}} p_{T,i} p_{T,j}$$

A typical QCD jet

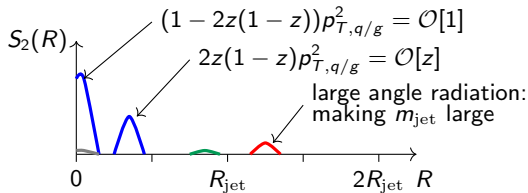
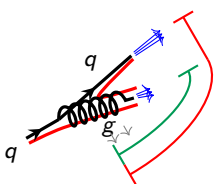
- Meanwhile, a typical QCD jet has a smoothly falling behavior according to the parton splitting kernels.



$$S_2(R; \Delta R) = \frac{1}{\Delta R} \sum_{\substack{i,j \in \text{jet} \\ R_{ij} \in [R, R+\Delta R]}} p_{T,i} p_{T,j}$$

A typical QCD jet

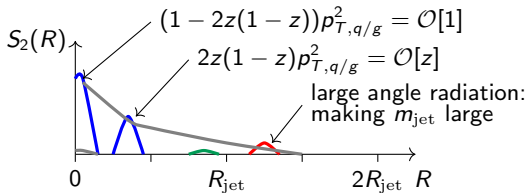
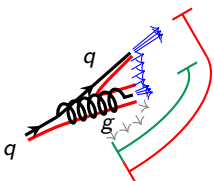
- Meanwhile, a typical QCD jet has a smoothly falling behavior according to the parton splitting kernels.



$$S_2(R; \Delta R) = \frac{1}{\Delta R} \sum_{\substack{i,j \in \text{jet} \\ R_{ij} \in [R, R+\Delta R]}} p_{T,i} p_{T,j}$$

A typical QCD jet

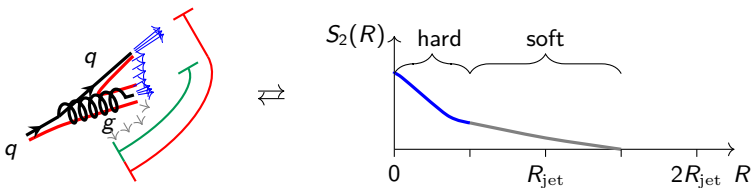
- Meanwhile, a typical QCD jet has a smoothly falling behavior according to the parton splitting kernels.



$$S_2(R; \Delta R) = \frac{1}{\Delta R} \sum_{\substack{i,j \in \text{jet} \\ R_{ij} \in [R, R+\Delta R]}} p_{T,i} p_{T,j}$$

A typical QCD jet

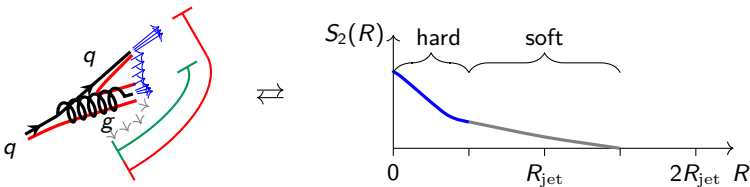
- Meanwhile, a typical QCD jet has a smoothly falling behavior according to the parton splitting kernels.



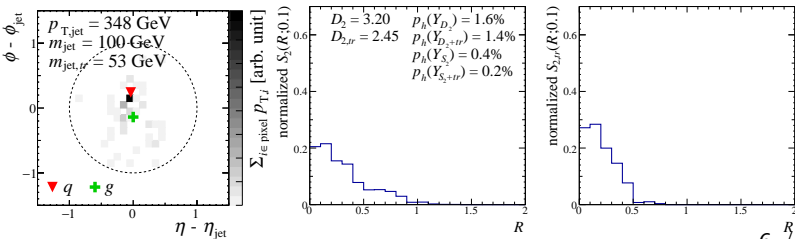
$$S_2(R; \Delta R) = \frac{1}{\Delta R} \sum_{\substack{i,j \in \text{jet} \\ R_{ij} \in [R, R+\Delta R]}} p_{T,i} p_{T,j}$$

A typical QCD jet

- Meanwhile, a typical QCD jet has a smoothly falling behavior according to the parton splitting kernels.



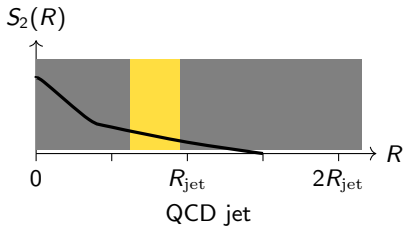
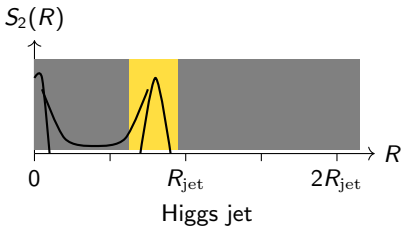
- This is a typical quark jet from MG5_aMC@NLO+Pythia8+Delphes.



Intermediate Check: a quick classifier between the Higgs jets and QCD jets

- The typical Higgs jets and QCD jets have a different spectrum. The energy deposit difference could be used as a quick classifier.

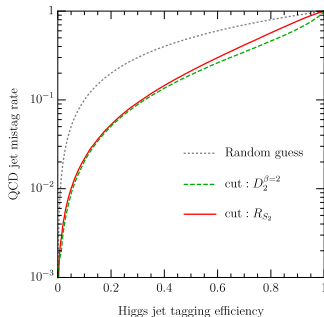
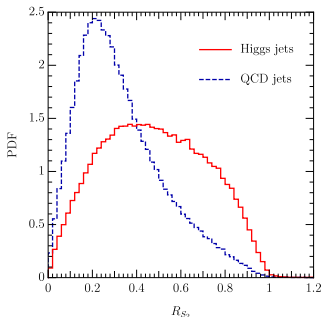
$$R_{S_2} = \frac{\int_{a\hat{R}_{b\bar{b}}}^{\min[a'\hat{R}_{b\bar{b}}, R_{\text{jet}}]} dR S_2(R)}{\int_0^{a\hat{R}_{b\bar{b}}} dR S_2(R) + \int_{\min[a'\hat{R}_{b\bar{b}}, R_{\text{jet}}]}^{\infty} dR S_2(R)}, \quad \hat{R}_{b\bar{b}} = \frac{2 \cdot 125 \text{ GeV}}{p_{T,\text{jet}}}$$



Intermediate Check: a quick classifier between the Higgs jets and QCD jets

- The typical Higgs jets and QCD jets have a different spectrum. The energy deposit difference could be used as a quick classifier.

$$R_{S_2} = \frac{\int_{a\hat{R}_{b\bar{b}}}^{\min[a'\hat{R}_{b\bar{b}}, R_{\text{jet}}]} dR S_2(R)}{\int_0^{a\hat{R}_{b\bar{b}}} dR S_2(R) + \int_{\min[a'\hat{R}_{b\bar{b}}, R_{\text{jet}}]}^{\infty} dR S_2(R)}, \quad \hat{R}_{b\bar{b}} = \frac{2 \cdot 125 \text{ GeV}}{p_{T,\text{jet}}}$$



- Event preselection: $m_{\text{jet}} \in [100, 150] \text{ GeV}$, and $p_{T,\text{jet}} \in [300, 400] \text{ GeV}$.

An Artificial Neural Network?

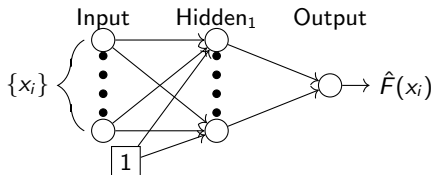
- Nevertheless, the energy deposit ratio of the spectrum is not the only information available in $S_2(R)$.
- We will introduce a neural network to use all the information available in $S_2(R)$.
- An artificial neural network is a mathematical model of a function.

$$\hat{F}(x_i) = v_j \cdot f(w_{ij} \cdot x_i + b_j)$$

where f is a nonlinear function, for example, we may consider ReLU,

$$f_{\text{ReLU}}(x) = \begin{cases} x & x > 0 \\ 0 & x \leq 0 \end{cases} \quad (1)$$

A graphical representation is follows.



- “Universal approximation theorem” states that if we have an enough number of the hidden neurons, which is the hidden dimension of j , then we can approximate any bounded continuous functions.

Our ANN setup

- Hence, we trained a neural network for the Higgs jet and QCD jet classification, and used the network as a classifier.

$$z_i^{(0)} = x_i$$

$$z_i^{(n)} = f_{\text{ReLU}}(w_{ij}^{(n)} z_j^{(n-1)} + b_i^{(n)})$$

$$\hat{y}_i = \exp[w_{ij}^{(5)} z_j^{(4)}] / \sum_i \exp[w_{ij}^{(5)} z_j^{(4)}]$$

- This network is trained for predicting a class vector

$$\vec{y} = \begin{cases} (1, 0) & \text{Higgs jet} \\ (0, 1) & \text{QCD jet} \end{cases}$$

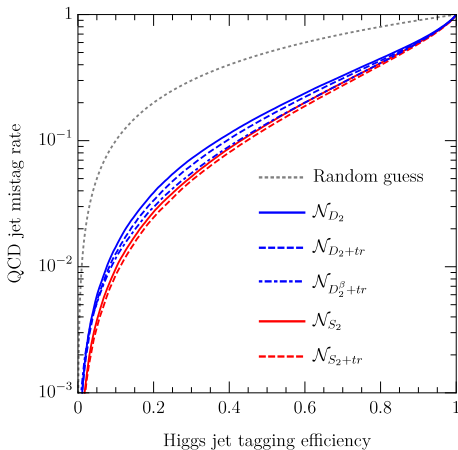
by minimizing the categorical cross entropy

$$L = - \sum_{\text{event}} \sum_i y_i \log \hat{y}_i$$

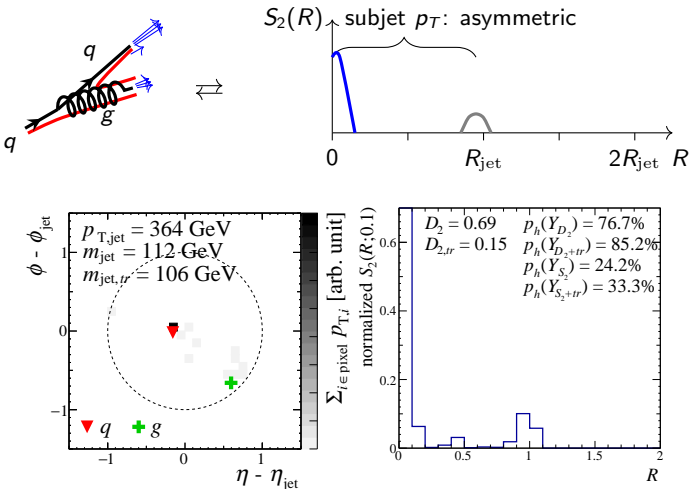
- The predicted class vector \hat{y} , which is the output of the neural network, can be used as a classifier.

Comparing $S_2(R)$ and D_2

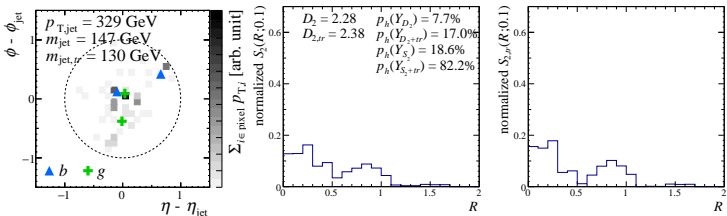
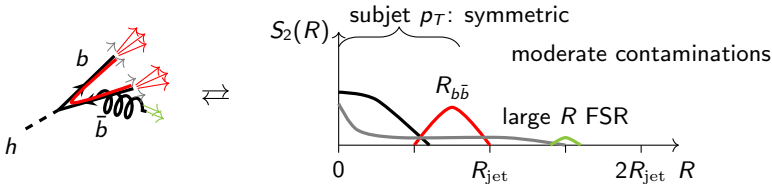
- To compare the information contained in $S_2(R)$ and D_2 , we compare the ROC curves of neural networks with following inputs.
- \mathcal{N}_{D_2} : $\{p_{T,\text{jet}}, m_{\text{jet}}, D_2^{\beta=2}\}$
- \mathcal{N}_{S_2} : $\{p_{T,\text{jet}}, m_{\text{jet}}, S_2(0; 0.1), \dots, S_2(1.9; 0.1)\}$
- $+tr$: trimmed variables are included.
- Q: what's the source of the difference?
 - Reduce mistagging
 - Going beyond two-prong



- Event preselection: $m_{\text{jet}} \in [100, 150]$ GeV, and $p_{T,\text{jet}} \in [300, 400]$ GeV.

A jet tagged in D_2 analysis only

- $\mathcal{N}_{D_2}: \{p_{T,\text{jet}}, m_{\text{jet}}, D_2^{\beta=2}\}$
- Even though this jet is two-prong, the likelihood for QCD jet is not that small.

A jet tagged in S_2 analysis with trimming only

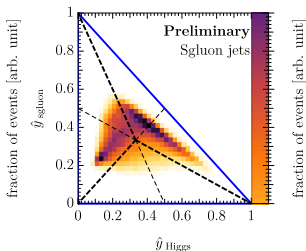
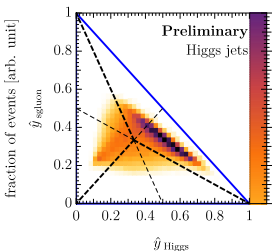
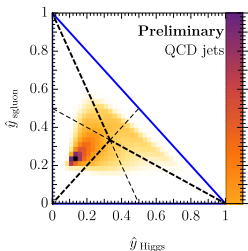
- This jet has two-prong substructure, but the subjects are wide and contaminated by other QCD activities.
- $S_2(R)$ together with jet trimming and a neural network can identify hard and soft substructure.

Color charge of the boosted Higgs jets

Preliminary

- $S_2(R)$ shows a good performance on identifying boosted Higgs jets from QCD jets.
- Is it possible to identify color charge of the Higgs jet from $S_2(R)$?
- We considered a color octet scalar, sgluon, decaying to $b\bar{b}$ and did a multi-class classification with a neural network \hat{y} predicting

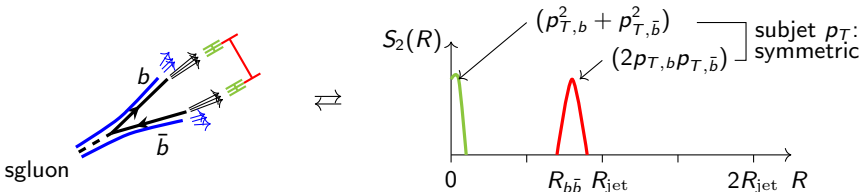
$$\vec{y} = \begin{cases} (1, 0, 0) & \text{Higgs jet} \\ (0, 1, 0) & \text{Sgluon jet} \\ (0, 0, 1) & \text{QCD jet} \end{cases}$$



A typical Sgluon jet

Preliminary

- The sgluon jet has a different radiation pattern compared to the Higgs jet because of its nontrivial color charge.

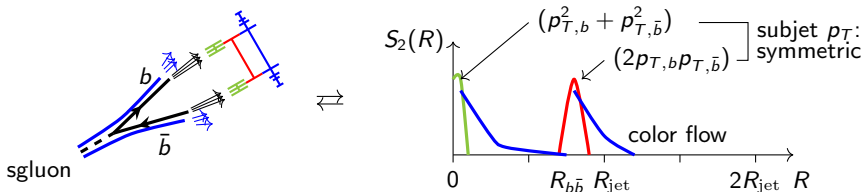


$$S_2(R; \Delta R) = \frac{1}{\Delta R} \sum_{\substack{i,j \in \text{jet} \\ R_{ij} \in [R, R+\Delta R]}} p_{T,i} p_{T,j}$$

A typical Sgluon jet

Preliminary

- The sgluon jet has a different radiation pattern compared to the Higgs jet because of its nontrivial color charge.

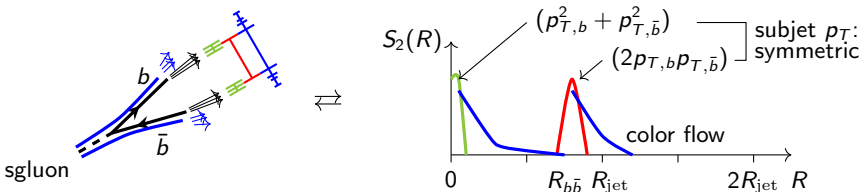


$$S_2(R; \Delta R) = \frac{1}{\Delta R} \sum_{\substack{i,j \in \text{jet} \\ R_{ij} \in [R, R+\Delta R]}} p_{T,i} p_{T,j}$$

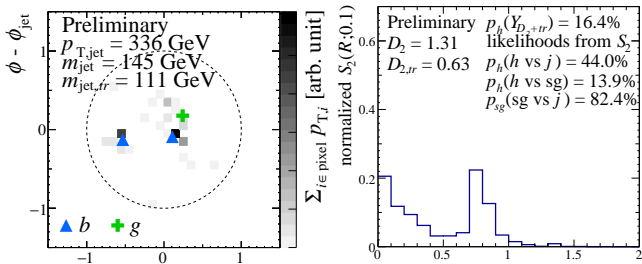
A typical Sgluon jet

Preliminary

- The sgluon jet has a different radiation pattern compared to the Higgs jet because of its nontrivial color charge.



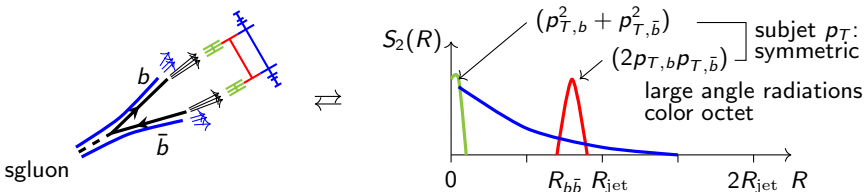
- This is a typical sgluon jet from MG5_aMC@NLO+Pythia8+Delphes.



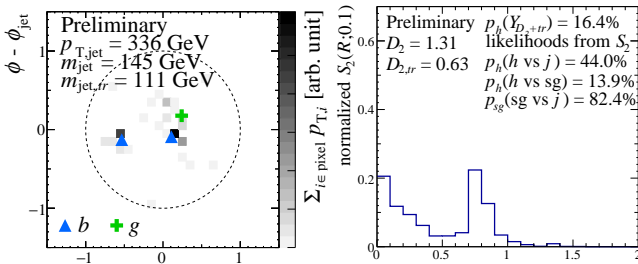
A typical Sgluon jet

Preliminary

- The sgluon jet has a different radiation pattern compared to the Higgs jet because of its nontrivial color charge.



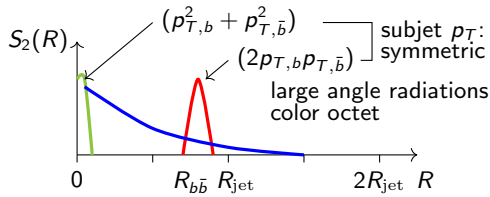
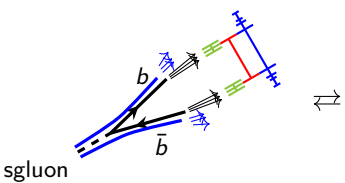
- This is a typical sgluon jet from MG5_aMC@NLO+Pythia8+Delphes.



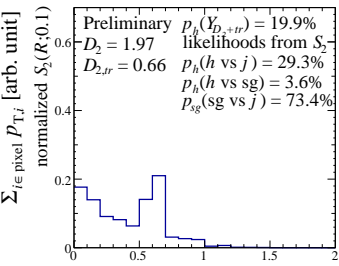
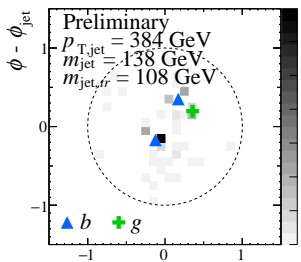
A typical Sgluon jet

Preliminary

- The sgluon jet has a different radiation pattern compared to the Higgs jet because of its nontrivial color charge.

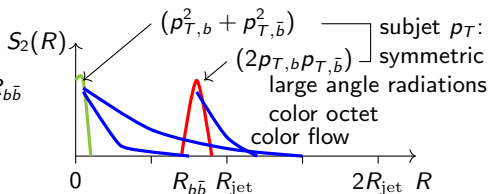
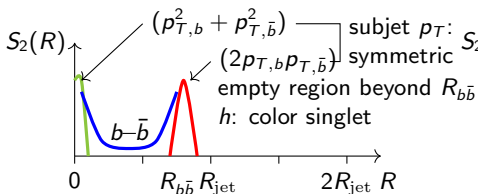


- This is a typical sgluon jet from MG5_aMC@NLO+Pythia8+Delphes.



Conclusion

- We have introduced a spectral analysis of jet substructure for classifying Higgs jets and QCD jets.
- The spectrum $S_2(R)$ is highly visual and useful in describing jet substructure with large angular scale.
- The improvement of performance of Higgs jet vs QCD jet classification is not large, but the spectral function $S_2(R)$ provide us a systematical framework for investigating jet substructure over various angular scale.
- For example, $S_2(R)$ can be used for understanding a color charge of boosted jets.



- There are more wider applications will be come out soon, so please stay tuned!

Backups

IRC safety of $S_2(R)$

- The $S_2(R)$ spectrum is better to be infrared and collinear (IRC) safe, namely invariant under soft and collinear radiations.

- Soft radiation: the parton radiates a $p_T = 0$ parton.

$$p_T \longrightarrow \begin{array}{c} \longrightarrow \\ \searrow \\ \swarrow \end{array} \quad \begin{array}{l} p_T \\ p_T = 0 \end{array}$$

- Collinear radiation: the parton splits in same direction \vec{R} .

$$p_T \longrightarrow \begin{array}{c} \longrightarrow \\ \longrightarrow \end{array} \quad \begin{array}{l} zp_T \\ (1-z)p_T \end{array}$$

- Otherwise, the virtual and real corrections in higher order perturbation theory do not sum up, and such a IRC unsafe observables are hard to be estimated from perturbative QCD calculations. (KNL theorem)

$$\text{---} \left(\text{loop} \right) \text{---} + \text{---} \left(\text{gluon} \right) \text{---} + \text{---} \left(\text{gluon} \right) \text{---} = \text{finite} \quad (2)$$

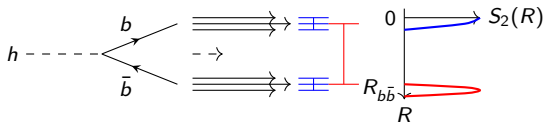
- $S_2(R)$ is IRC safe because soft or collinear radiation does not introduce any new angular scale R .

IRC safety of $S_2(R)$

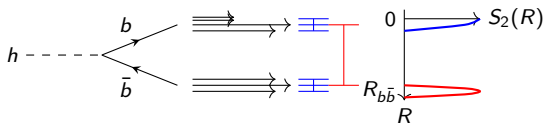
- The $S_2(R)$ spectrum is IRC safe.

$$S_2(R; \Delta R) = \frac{1}{\Delta R} \sum_{\substack{i,j \in \text{jet} \\ R_{ij} \in [R, R+\Delta R]}} p_{T,i} p_{T,j}, \quad (3)$$

- Soft radiation is ignored safely because $p_{T,i} p_{T,j} = 0$ if i or j is a soft radiation.



- Collinear radiation is okay because \vec{R} does not change and the radiation products always sum up.



Comparison to another variable

- For comparison, we prepare an ANN analysis with D_2 variable (1409.6298)

$$e_2^\beta = \frac{1}{p_{T,\text{jet}}^2} \sum_{\substack{i,j \in \text{jet} \\ i < j}} p_{T,i} p_{T,j} R_{ij}^\beta, \quad (4)$$

$$e_3^\beta = \frac{1}{p_{T,\text{jet}}^3} \sum_{\substack{i,j,k \in \text{jet} \\ i < j < k}} p_{T,i} p_{T,j} p_{T,k} R_{ij}^\beta R_{jk}^\beta R_{ki}^\beta, \quad (5)$$

$$D_2^\beta = \frac{e_3^\beta}{(e_2^\beta)^3} \sim \frac{\Delta}{(-)^3}, \quad (6)$$

- For Higgs jets, D_2 is small because three-point energy correlation have to count soft or collinear radiation.

$$D_2^\beta \approx \frac{\text{triangle}}{(-)^3} \approx \frac{\text{blue line}}{\text{red line}} \ll 1$$

